Iranian Journal of Astronomy and Astrophysics
Vol. 12, No. 3, Summer 2025, 209–225
©Available online at http://ijaa.du.ac.ir
DOI: 10.22128/ijaa.2025.3140.1229
Online ISSN: 2383–403X

Iranian Journal of Astronomy and Astrophysics

Review Paper

Numerical Modeling of the Solar Wind: Fluid, Kinetic, and Hybrid Approaches

Somayeh Taran
Faculty of Physics, University of Tabriz, PO Box 51666-16471, Tabriz, Iran;
E-mail: taran@tabrizu.ac.ir

Received: 11 November 2025; **Accepted:** 19 December 2025; **Published:** 22 December 2025

Abstract. This paper provides a comprehensive overview of the numerical methods used to model the solar wind, integrating fluid, kinetic, and hybrid perspectives. Beginning with the foundations of solar wind theory and the development of magnetohydrodynamic (MHD) models, we discuss how fluid-based formulations enable the simulation of global structures such as coronal mass ejections, shocks, and large-scale variations in the heliospheric magnetic field. To address processes that fall outside the scope of MHD, we examine kinetic modeling based on the Vlasov–Maxwell equations, emphasizing its capability to reproduce non-Maxwellian particle distributions, wave–particle interactions, temperature anisotropies, and collisionless heating. Hybrid approaches that merge MHD with kinetic techniques are highlighted as essential tools for capturing the multi-scale nature of the solar wind, particularly in regions where macroscopic flows couple to microphysical dynamics. The paper further reviews major numerical strategies used in solar wind simulations, comparing explicit and implicit time integration, adaptive mesh refinement, Particle-in-Cell (PIC) methods, and semi-Lagrangian approaches. Key stability considerations—including boundary-condition selection, the Courant–Friedrichs–Lewy (CFL) constraint, appropriate spatial and velocity-space resolution, and the targeted use of artificial diffusion—are discussed in relation to their impact on accuracy and robustness. Example simulations demonstrate the ability of advanced models to reproduce observed proton and electron temperature profiles from the Sun out to 1AU. Overall, numerical modeling plays a central role in interpreting solar wind observations and predicting space-weather conditions, and ongoing advances in computational methods continue to strengthen our understanding of heliospheric plasma dynamics.

Keywords: Solar Wind, Numerical Solution, MHD, Kinetic.

1 Introduction

The solar wind is a continuous outflow of plasma from the Sun's corona, filling the heliosphere with a stream of charged particles. Understanding how this flow evolves is essential for forecasting space weather, protecting satellites, and enabling human activity in space [1–5]. Our modern understanding of the solar wind can be traced back to Eugene Parker's influential work in 1958, which demonstrated that the Sun must constantly release material into interplanetary space [6]. Since then, both magnetohydrodynamic (MHD) and kinetic models have become indispensable tools for exploring the physics of the solar wind [7–10].

MHD provides the backbone for studying large-scale solar wind behavior. By treating the plasma as a conducting fluid governed by the continuity, momentum, energy, and induction equations [11], MHD models allow us to simulate global heliospheric structures, including the evolution of coronal mass ejections (CMEs), which exert a profound influence on space-weather conditions throughout the solar system [6,12].

However, as research progressed into the early 2000s, it became clear that MHD alone cannot fully explain the complexity of the solar wind. Many essential processes—such as particle acceleration, temperature anisotropies, and wave–particle interactions—are fundamentally kinetic in nature [13–17]. Kinetic models, which follow the behavior of individual charged particles, are therefore critical for understanding small-scale structures, collisionless shocks, and energetic particle dynamics [7,18–20]. Hybrid approaches later emerged, combining MHD for large-scale behavior with particle-in-cell (PIC) methods to resolve kinetic physics [21–23].

Waves are central to both the MHD and kinetic perspectives of solar-wind physics. Numerous wave modes—Alfvén, magnetosonic, kink, kinetic Alfvén, whistler, ion-acoustic, and Langmuir waves—transport energy, heat particles, influence turbulence, generate shocks, and shape the magnetic structure of the heliosphere [24–36]. These wave-driven mechanisms are fundamental to understanding and predicting space weather.

Advances in numerical methods have played a pivotal role in enabling increasingly sophisticated solar-wind models. Early computational work in the 1970s relied on finite-difference and finite-volume techniques capable of solving the MHD equations. By the 1980s and 1990s, more advanced algorithms—such as Roe solvers, Godunov methods, and other shock-capturing schemes—enabled more realistic simulations of nonlinear solar-wind evolution [37,38]. These improvements allowed researchers to investigate the structure of the heliosphere and explore how the solar wind interacts with planetary magnetospheres [39–42].

In recent years, high-order numerical schemes and adaptive strategies have become increasingly important. Discontinuous Galerkin methods, adaptive mesh refinement (AMR), and high-resolution finite-volume techniques now support accurate multi-scale simulations of the corona and heliosphere. Modern global MHD frameworks—including MAS, ENLIL, AWSoM, and EUHFORIA—leverage these tools to model the solar wind in both research and operational contexts [43–48]. These systems incorporate realistic boundary conditions and physically motivated heating and acceleration mechanisms, significantly enhancing our ability to simulate the solar wind from its origin in the corona out to interplanetary space. Despite these advances, accurately representing particle distribution functions remains a persistent challenge. Standard assumptions–such as Maxwellian or bi-Maxwellian distributions–often fail to capture the non-thermal and non-equilibrium nature of the solar wind, especially near the Sun, where kappa-type distributions are frequently observed [49]. Transient events such as shocks and solar flares can further introduce strong anisotropies and rapid changes in particle populations [50–52]. Because the solar wind is highly dynamic and far from equilibrium, static distribution-function assumptions frequently fall short. Modern multi-scale modeling efforts aim to bridge these gaps by coupling large-scale MHD frameworks with embedded kinetic regions. These hybrid systems provide a more complete description of solar-wind behavior, allowing models to capture both global heliospheric structures and the small-scale kinetic processes that shape them.

2 Solar wind MHD model

Magnetohydrodynamics (MHD) is a theory that uses magnetism, fluid dynamics, and thermodynamics to study how electrically conducting fluids like plasma behave. In the mid-20th century, the MHD equations were first developed, providing the mathematical framework necessary for the study of plasma in space. Initial work focused on the theoretical formulation of MHD and its implications for astrophysical phenomena, and its implications for astrophysical phenomena [53]. The basic Formulation of MHD Equations is as follows,

- **Continuity Equation**

$$\frac{\partial \rho}{\partial t} + \nabla \cdot (\rho \mathbf{v}) = 0, \tag{1}$$

  where ρ is the mass density and $\mathbf{v}$ is the velocity field of the plasma.

- **Momentum Equation**

$$\rho \frac{d\mathbf{v}}{dt} = -\nabla P + \rho \mathbf{g} + \mathbf{J} \times \mathbf{B} + \mathbf{F}_\nu, \tag{2}$$

  where P is the pressure, $\mathbf{g}$ represents gravitational effects, $\mathbf{J} = \nabla \times \mathbf{B}/\mu_0$ is the current density, $\mathbf{B}$ is the magnetic field, and $\mathbf{F}_\nu$ is the viscosity term.

- **Induction Equation**

$$\frac{\partial \mathbf{B}}{\partial t} = \nabla \times (\mathbf{v} \times \mathbf{B}) + \eta \nabla^2 \mathbf{B}, \tag{3}$$

  where η is the magnetic diffusivity.

- **Energy Equation**

$$\frac{dE}{dt} = -P\nabla \cdot \mathbf{v} + \nabla \cdot (\kappa \nabla T) + Q, \tag{4}$$

  where E is the total energy density, κ is the thermal conductivity, T is temperature, and Q represents external heating sources. Various formulations exist depending on the plasma equation of state and all sources and sinks of energy [54].

MHD solar wind modeling assumes that the solar wind behaves like a compressible, viscous, and electrically conductive fluid. To enhance the accuracy of modeling the solar corona and the acceleration of the solar wind, the effects of gravity are frequently incorporated. Additionally, the presence of magnetic fields is essential, as they play a key role in governing the dynamics of both the solar atmosphere and the solar wind [7,55,56].

In the context of numerical methods for addressing MHD equations in solar wind modeling, both finite difference and finite volume methods have their respective advantages and limitations. The decision regarding which method to use typically hinges on the specific needs of the simulation and the characteristics of the problem at hand. In the late 1980s and throughout the 1990s, researchers started to adopt finite volume methods, which provided an improved approach to managing discontinuities compared to conventional finite difference methods whose studies were limited to two dimensions [57–59]. Given the inherent three-dimensional (3D) characteristics of geomagnetic space, 3D MHD simulations began to develop in the 1980s [60–62]. MHD simulations have played a crucial role in enhancing our understanding of the dynamics of CMEs, particularly regarding their movement through the solar wind and their interactions with Earth's magnetosphere [63–69]. Using MHD simulations, researchers investigated how shock waves form in the solar wind, particularly examining the dynamics of fast solar wind streams and their interactions with slower streams and CMEs. These studies contribute to a better understanding of the complex structure of the interplanetary magnetic field, including the magnetic configurations of solar wind streams and their influence on space weather phenomena [34,42,70–72]. MHD simulations illustrate the variations in solar wind properties throughout the solar cycle, emphasizing the connection between solar activity, such as sunspots, and the features of the solar wind [73–75].

Recent initiatives have involved high-resolution global MHD simulations that utilize cutting-edge computing resources. These simulations offer in-depth understanding of the solar wind's structure and its reactions to solar events. ENLIL is a three-dimensional MHD model of the heliosphere that operates over time and computes the plasma MHD equations through a Flux-Corrected Transport (FCT) algorithm. It was created by NASA that simulate the solar wind as it travels from the sun (21.5 or 30 solar radii) to the distant outer regions of the heliosphere (such as 2 AU to encompass both Earth and Mars, 5 AU for Ulysses, or 10 AU for Cassini) [9,76]. The Block-Adaptive-Tree-Solarwind-Roe-Upwind-Scheme (BATSRUS) code computes 3D MHD equations in a finite volume format, employing numerical techniques associated with Roe's Approximate Riemann Solver. BATSRUS is a robust, generalized MHD code featuring adaptive mesh refinement, which allows it to be tailored for solving the governing equations of both ideal and resistive MHD [77–79]. Also, Flux Corrected Transport is a robust numerical technique that improves the stability and precision of advection schemes in fluid dynamics. It offers a means to preserve physical fidelity when dealing with steep gradients or sharp features in the transported quantity. By integrating prediction and correction, this method adeptly addresses the challenges associated with advection-dominated problems [80,81].

3 Solar wind kinetic model

Kinetic theory is essential for understanding the dynamics of the solar wind, which is the continuous flow of charged particles from the solar corona into space. The kinetic approach provides insight into the microphysical processes that govern the behavior of plasma in the solar wind, including the formation of energy distributions, instabilities, and wave-particle interactions [7,15,82]. Kinetic theory employs distribution functions to describe the statistical behavior of particles within the solar wind. These functions explain how particle velocities are distributed and how they evolve. The mathematical framework of the kinetic theory of solar wind consists of a combination of differential equations and numerical techniques aimed to describe the behavior of charged particles in the plasma. The theory is based on the Vlasov equation, which considers the distribution function of particles,

$$\frac{\partial f_s}{\partial t} + \mathbf{v}.\nabla f_s + \frac{e_s}{m_s}\left(\mathbf{E} + \frac{\mathbf{v} \times \mathbf{B}}{\mathbf{c}}\right).\nabla_v f_s = 0, \tag{5}$$

where $\mathbf{E}(\mathbf{r}, t)$, $\mathbf{B}(\mathbf{r}, t)$, f_s, e_s are the average of the electric and magnetic fields, distribution function, and charged particle, respectively. Kolsrud in 1958 [83], used the 5 equation and the set of Maxwell equations (6) and formulated the collisionless MHD model,

$$\nabla \times \mathbf{B} = 4\pi \sum_s \frac{e_s}{c} \int f_s v d^3v + \frac{1}{c}\frac{\partial \mathbf{E}}{\partial t}, \tag{6}$$

$$\nabla.\mathbf{E} = 4\pi \sum_s e_s \int f_s d^3v,$$
$$\frac{\partial \mathbf{B}}{\partial t} = -c\nabla \times \mathbf{E},$$
$$\nabla.\mathbf{B} = 0.$$

Solving the above set of equations with seven independent variables $(t, \mathbf{v}, \mathbf{r})$ is very difficult. Therefore, by expanding both sides of the Vlasov equation in terms of ρ_c/L we can reduce the number of effective variables in the kinetic equation to two. ρ_c is the cyclotron radius and L is the macroscopic scale length of the plasma. In the case of the lowest remaining orders, the particle velocity will consist of two components parallel and perpendicular to the magnetic field ($\mathbf{E} \times \mathbf{B}$).
To begin the plasma formulation, the distribution function (f), magnetic field (B), and electric field (E) were expanded in terms of $1/e$ (electron charge). For example, the distribution function was taken as $f = f_0 + f_1$ where $f_1 = \mathcal{O}(1/e)$ is the perturbation of the distribution function. This is equivalent to considering all frequencies in the problem to be lower than the cyclotron frequency, Ω, and the plasma frequency, ω_p. [84,85].
With the calculations done, the kinetic equation for each particle in terms of the zeroth order distribution function ($f_{0s}(v_\parallel, \mu, \mathbf{r}, t)$) will be as follows,

$$\frac{\partial}{\partial t}(f_s B) + \nabla.[f_s B(v_\parallel \hat{\mathbf{b}} + \mathbf{v}_E)] + \frac{\partial}{\partial v_\parallel}[f_s B(-\hat{\mathbf{b}}.\frac{D\mathbf{v}_E}{Dt} - \mu\hat{\mathbf{b}}.\nabla B + \frac{e_s E_\parallel}{m_s})] = 0, \quad (7)$$

e_s and m_s denote the charge and mass of each particle, respectively, and $v_\parallel = \hat{\mathbf{b}}.\mathbf{v}$ $v_E = c(\mathbf{E}\times \mathbf{B})/B^2$, $\mu = \frac{v_\perp^2}{2B}$,$\hat{\mathbf{b}} = \mathbf{B}/B$, $D/Dt = \partial/\partial t + (v_\parallel \hat{\mathbf{b}} + v_E).\nabla$,.. the parallel and perpendicular signs indicate the directions parallel and perpendicular to the magnetic field, and μ is the magnetic moment, and $E_\parallel$ is the parallel component of the electric field. With the particle distribution function known, the different momenta of the velocity space are defined as follows, Calculating the moments of different orders of this Equation 7 yields the set of equations for non-collision plasma [86,87].

Although the solar wind consists of a low-density plasma, collision processes are usually weak but may influence the distribution of particles. Landau damping, a phenomenon in which oscillations in plasma may diminish due to the collective effects of particles, can be important in the solar wind [82,88]. The interaction of particles with electromagnetic waves can cause heating and the acceleration of solar wind particles. Kinetic models are capable of investigating how these interactions happen in the context of the solar wind environment [89] and aids in comprehending plasma instabilities that may occur in the solar wind and impact wave generation, including ion-acoustic instability or kinetic Alfvén wave instability [90–92].

Different numerical techniques, including finite difference methods, spectral methods, and Particle-In-Cell (PIC) simulations, are used to solve the Vlasov equation and Maxwell's equations simultaneously numerically. Semi-Lagrangian techniques and Monte Carlo simulations can also be employed to investigate plasma dynamics [93–95]. Numerical methods for the Vlasov equation have been applied to investigate the effects of different plasma waves on particle distributions, yielding insights into solar wind turbulence [96–99]. Kinetic treatments of solar wind interactions with planets' magnetospheres have provided a framework for understanding magnetic reconnection events. Numerical simulations demonstrate the interaction between the solar wind and planetary magnetic fields, providing insights into space weather phenomena [100–102]. Advanced kinetic models have been developed to investigate the solar wind's interaction with the interstellar medium. These models help understand the heliosphere structure and its boundary with interstellar space [103–105].

4 Numerical schemes in the solar wind

Numerical techniques for solving the differential equations that describe the dynamics of the solar wind are crucial for effectively modeling its behavior and comprehending different physical phenomena. The solar wind is typically characterized by a series of MHD equations, kinetic equations, or hybrid models that integrate both fluid and kinetic aspects. The selection of a numerical approach is influenced by the characteristics of the differential equations, the level of accuracy required, and the computational resources at hand.

There are two general explicit and implicit methods that are both widely used for solving partial differential equations. Every method has its specific strengths and weaknesses, especially when considering the distinct challenges presented by the behavior of the solar wind, including non-linear interactions, wave propagation, and the formation of shocks. In explicit methods, the solution for the next time step is derived directly from the information available at the current time step. The update formula involves previous time points, allowing for straightforward computation. Many explicit methods (like standard finite difference schemes) can be limited by a stability condition. This requires sufficiently small time steps for stability, which can lead to high computational costs in large simulations. Explicit methods are generally employed in problems where the solution behaves smoothly and does not involve stiff dynamics. This is particularly relevant in solar wind MHD simulation, where simplicity and ease of implementation are advantageous. In kinetic simulations of the solar wind, explicit integration methods can be used to follow particle trajectories and compute distribution functions [82,106,107]. Implicit methods require solving a system of equations at each time step, often resulting in substantial linear systems that need to be addressed iteratively. The upcoming time step relies on both present and future values, which may enable the use of larger time steps. Implicit methods can provide unconditional stability for specific types of problems and are commonly used in simulations that involve strong gradients, shocks, and various stability challenges. They are effective at managing the intricate dynamics present in solar wind environments. These methods offer benefits when addressing multi-fluid equations that characterize various species found in the solar wind.

To numerically solve differential equations, it is necessary to discretize them. The choice of discretization method can lead to varying levels of discretization error, and it is essential to strive for the lowest error possible by selecting the most effective method. Reducing the size of the grid cells will also minimize the discretization error:

4.1 Finite Volume Methods (FVM)

It divides the space into small cells and calculates the average of each parameter by transforming the differential equations into their integrals within each cell. This method, considering a finite volume around each node on the generated grid, converts the volume integrals in the partial differential equations into surface integrals using the divergence theorem and calculates the flux passing through the surfaces of each element of the volume. For this reason, this method is practically conservative and ideal for simulating shock waves and discontinuities in the solar wind. The main disadvantages of this method are the difficulty of using it for spatial accuracies higher than the second order and the complexity of representing the second-order derivatives in space. It is particularly suitable for hyperbolic equations like those in MHD.

4.2 Finite Difference Methods (FDM)

The finite Difference Method is one of the simplest methods for discretizing differential equations introduced by Euler. It is commonly used to solve partial differential equations by approximating derivatives with difference equations. These methods are straightforward to implement and work well for problems with well-defined boundary conditions. Considering one-dimensional functions, the Taylor expansion of an arbitrary function ϕ about a point x_i is defined as follows,

$$\phi(x) = \phi(x_i) + (x - x_i)(\frac{\partial \phi}{\partial x})_i + \frac{(x - x_i)^2}{2!}(\frac{\partial^2 \phi}{\partial x^2})_i + ... + \frac{(x - x_i)^n}{n!}(\frac{\partial^n \phi}{\partial x^n})_i. \tag{8}$$

By transforming the Equation 8 into the following form, the spatial derivative of the function ϕ in the finite difference approximation is obtained,

$$(\frac{\partial \phi}{\partial x})_i = \underbrace{\frac{\phi_{i+1} - \phi_i}{x_{i+1} - x_i}}_{\text{FDM}} \underbrace{- \left(\frac{(x - x_i)}{2!}(\frac{\partial^2 \phi}{\partial x^2})_i + ... + \frac{(x - x_i)^{n-1}}{n!}(\frac{\partial^n \phi}{\partial x^n})_i \right)}_{\text{Discretization error}}. \tag{9}$$

Discretization error arises from using the limited part of the Taylor series in the decomposition. If the Taylor expansion is expanded around different nodes x_{i-1} and x_{i+1} or around both of these nodes, the approximation of the finite difference method and the order of accuracy of each method will be as follows,

- Forward Difference Scheme (FDS)

$$(\frac{\partial \phi}{\partial x})_i \approx \frac{\phi_{i+1} - \phi_i}{x_{i+1} - x_i}, \qquad \mathcal{O}(\Delta x).$$

- Backward Difference Scheme (BDS)

$$(\frac{\partial \phi}{\partial x})_i \approx \frac{\phi_i - \phi_{i-1}}{x_i - x_{i-1}}, \qquad \mathcal{O}(\Delta x).$$

- Central Difference Scheme (CDS)

$$(\frac{\partial \phi}{\partial x})_i \approx \frac{\phi_{i+1} - \phi_{i-1}}{x_{i+1} - x_{i-1}}, \qquad \mathcal{O}(\Delta x)^2.$$

Due to the high accuracy of the central difference scheme discretization compared to other methods, this method is more suitable for discretizing spatial derivatives in equations [108]. The FDM method can suffer from numerical diffusion and may require careful time-stepping to ensure stability.

4.3 Spectral Methods

The spectral method represents the solution as a series of basis functions, typically using Fourier or Chebyshev polynomials, which provides high accuracy for smooth problems. It converts differential equations into spectral space, simplifying the resolution process. Once solved, the solution is transformed back into physical space. However, this approach tends to perform poorly in situations involving sharp gradients or discontinuities, such as shocks [109].

4.4 Particle-In-Cell (PIC)

The PIC method combines Lagrangian and Eulerian approaches, allowing for the simulation of charged particle dynamics in electromagnetic fields. For its implementation particles are tracked through the simulation domain, interacting with grid-based fields calculated from Maxwell's equations. This method effectively captures kinetic effects and wave-particle interactions, making it suitable for modeling the solar wind's complex behavior [110].

4.5 Adaptive Mesh Refinement (AMR)

AMR techniques adaptively refine the grid based on solution features, which is particularly useful for solving partial differential equations with varying scales, such as in the solar wind. In this method meshes are refined in regions with high gradients (e.g., near shocks) and coarsened elsewhere, helping to optimize computational resources. It is more challenging to implement and oversee than standardized methods [111].

4.6 Iterated Crank-Nicolson

The Crank-Nicolson method is a popular numerical technique for addressing partial differential equations, especially in time-dependent scenarios, and is particularly valuable in situations where stability and accuracy are crucial [112,113]. Regarding solar wind numerical solutions, the Crank-Nicolson method is typically applied to resolve the MHD equations, which outline the dynamics of plasma in the solar wind and other hydrodynamic models of plasma flows [114,115]. The iterative Crank–Nicholson method is an explicit version of the Crank–Nicholson method that converts the implicit method into an explicit algorithm by successive iterations. This method was proposed by Tekolski, who considered that using two iterations is sufficient to obtain the correct solution [116,117]. The iterative Crank-Nicholson method operates based on prediction, correction, and interpolation of quantities, achieving second-order accuracy in both time and space [87,118].

Solar wind parameters near the solar surface change rapidly. For this purpose, it is better to use a logarithmic grid, which increases the size of the grid cells with increasing distance from the solar surface. It is highly accurate in examining parameters with very rapid changes. Figure 1 shows an example of a one-dimensional logarithmic grid.

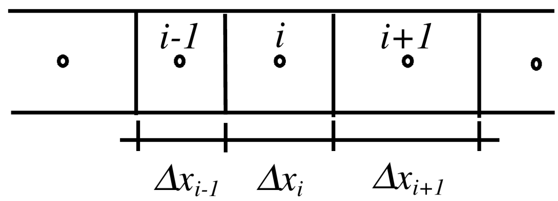

Figure 1: A demonstration of the logarithmic division of space.

5 Stability of numerical method

In addition to the impact of choosing a numerical method on maintaining simulation stability, inaccurate selected boundary conditions can result in numerical instabilities, particularly at the model's inner or outer boundaries. For instance, applying unrealistic boundary conditions—like fixed velocities or pressures that do not align with the physical environment—can create unphysical reflections that disrupt the solution [119]. A stable algorithm does not increase the error across different computational steps. One of the most important stability conditions in numerical calculations is the Courant-Friedrichs-Levy (CFL) condition, which is applicable in various physical scenarios. This condition appears in explicit numerical calculations and is defined in one dimension as follows,

$$C = \frac{u\Delta t}{\Delta x}, \tag{10}$$

Where the dimensionless number C is called the Courant Number. Δx and Δt represent the spatial and temporal steps, respectively. u is the medium's velocity, which in hydrodynamics is equal to the speed of sound and in magnetohydrodynamics is equal to the Alfv́en speed. The Courant number is a quality that expresses how much information is transmitted through a network in a time step. If the Courant number is greater than one, it means that information propagation occurs in each step more than one cellular network. In this case, the time integrator does not have the opportunity to interpret the physical phenomenon that has happened and the so-called solution will be unstable, so this number cannot be greater than one in the explicit method. Explicit time-stepping methods limit the time step based on the spatial grid size, leading to a small Courant number. In many cases, this restricts the time step and may slow down simulations. Implicit methods allow for larger time steps, but they may require more computational resources [120].

The spatial resolution of the grid is a crucial element influencing stability. To accurately capture smaller-scale features of the solar wind, such as turbulence or kinetic effects in hybrid or kinetic models, higher resolution grids are essential. Conversely, low-resolution grids may result in an inadequate sampling of wave modes and numerical diffusion, which can decrease the solution's accuracy and stability [56,121]. In kinetic and hybrid models, the stability of simulations is significantly influenced by the precise resolution of wave-particle interactions (such as Alfv́en waves and Whistler waves) and the kinetic behavior of particles. A fine balance between spatial and velocity space resolution is the requirement of simulation stability. If these interactions are not managed properly, numerical artifacts like particle trapping or unrealistic heating may occur [121,122]. The solar wind spans a wide range of time scales, from fast Alfv́en waves propagating on short time scales to slower kinetic processes like ion heating. If these time scales are not adequately represented in the simulation, it may result in numerical artifacts or the inability to identify crucial physical phenomena, including turbulence or the development of shocks [82,123]. Another important parameter for the stability of some numerical methods and also to prevent the occurrence of unphysical fluctuations in the numerical solution results is the addition of artificial diffusion terms to the existing differential equations. These terms are added to the right side of each equation as the second derivative of the main quantity present in each equation and with a constant and positive coefficient ($-D\frac{\partial^2\psi}{\partial x^2}$) [87].

A one-dimensional simulation of solar winds using the Crank-Nicholson method is illustrated in Figures 2 and 3. The observational results are consistent with the temperature changes of electrons and protons observed at the distance from the Sun to Earth. In the two-fluid solar wind model, the electron distribution is characterised as kappa-Maxwellian and the proton distribution is modelled as bi-Maxwellian. The temperature of electrons is illustrated for various values of the kappa function index [87].

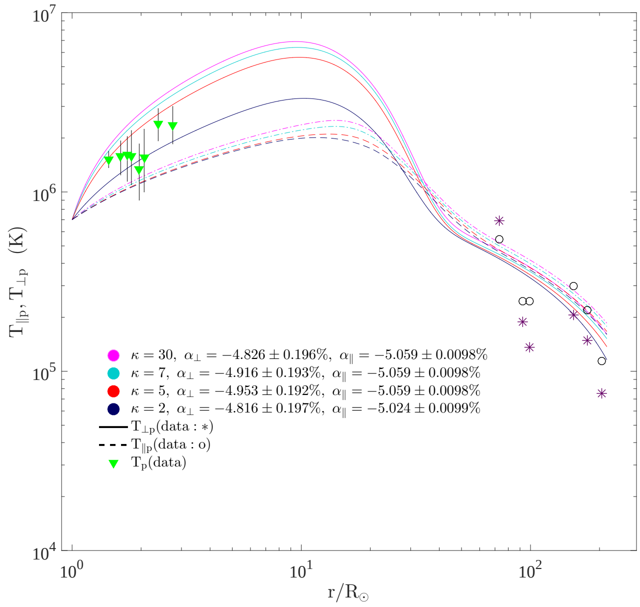

Figure 2: The solid lines represent the perpendicular temperature and the dashed lines represent the parallel temperature for protons for $\kappa = 2, 5, 7$, and 30 vs the distance from the Sun. The ($*s$) and ($\circ s$) show the *Helios* data reported for parallel and perpendicular temperatures for the fast solar wind, respectively [124], the ($\blacktriangledown s$) show the UVCS/*SoHO* data for the proton temperature, the power-law indices ($\alpha_\perp$,$\alpha_\parallel$) for all κ are presented.

6 Conclusion

Numerical techniques for addressing solar wind differential equations are a crucial component of space physics research. Scientists can obtain essential insights into solar wind behavior and its effects on space weather and planetary atmospheres by utilizing advanced computational techniques. Different methods can be employed to numerically solve solar wind dynamics, each presenting its own set of benefits and drawbacks. Conventional techniques like finite difference, finite element, and spectral methods offer robust frameworks for solving the governing equations of the solar wind, which include the MHD equations. These techniques enable comprehensive simulations of the solar wind's characteristics, starting from its source on the Sun to its interaction with planetary magnetospheres. MHD models are extensively utilized for large-scale simulations, providing computational efficiency when addressing the solar wind's macroscopic behavior, including its interaction with the magnetic field. These models successfully represent the overall dynamics, including shock formation, turbulence, and solar wind acceleration, but might be deficient in accounting for intricate microphysical processes. Conversely, kinetic theory models, including the Vlasov or Particle-In-Cell (PIC) methods, provide a more intricate, microscopic perspective of the plasma, especially valuable for comprehending subtle phenomena such as wave-particle interactions and kinetic instabilities. However, they entail increased computational costs and complexity. Both methods are crucial for a comprehensive understanding of the solar wind, and hybrid models that integrate MHD and kinetic approaches are being investigated to

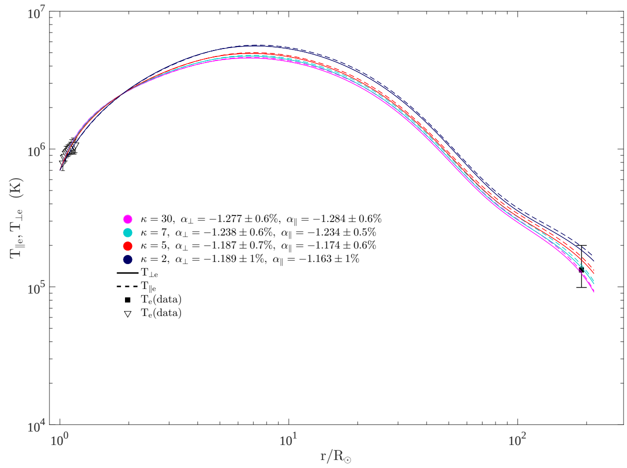

Figure 3: The solid lines are perpendicular temperature and the dashed lines are the parallel temperature for electrons for $\kappa = 2, 5, 7$, and 30 from the Sun to the Earth. The ($\triangledown s$) show the $SoHO$/SUMER data of electron temperature in a polar coronal hole [125] and the square (■) is the mean electron temperature for the fast solar wind that measured by ISEE 3 and *Ulysses* [126]. $\alpha_\perp$ and $\alpha_\parallel$ are the power-law indices for $\kappa = 2, 5, 7$, and 30 at (0.3 - 1)AU.

harness the advantages of each. Recent developments in computational methods, including hybrid models that merge kinetic and MHD approaches, as well as advanced particle-based techniques like the Particle-in-Cell (PIC) method, have facilitated more precise modeling of the small-scale, non-ideal effects impacting solar wind dynamics. These techniques are especially effective in capturing phenomena such as turbulence, shock formation, and interactions with interplanetary magnetic fields, which are frequently difficult to model using traditional MHD methods. Employing explicit methods in solar wind simulations offers straightforwardness and ease of application, but may require smaller time intervals to ensure stability. On the other hand, implicit methods permit larger time steps and are more stable when faced with complexity and stiff dynamics, although they necessitate more advanced solvers and increased computational resources. Researchers can choose the most suitable method based on the specific application and needs of the simulation (e.g., resolution, accuracy, computational budget). The solar wind includes the transmission of shocks, like Alfvén shocks and termination shocks, as well as discontinuities. It is essential for numerical methods to manage these elements effectively, avoiding any unintended oscillations or instabilities. Therefore, the creation of shock-capturing algorithms is vital for ensuring stability. The stability of numerical solutions in solar wind models is a key factor in ensuring the accuracy and reliability of the predictions. Numerical instabilities can arise from issues such as poor resolution, improper boundary conditions, inadequately resolved time scales, or failure to handle nonlinear wave-particle interactions. Addressing these stability issues involves choosing the right numerical method, ensuring proper resolution, and applying appropriate boundary conditions that reflect the physical environment of the solar wind. Ongoing improvements in numerical methods and computational techniques are necessary to enhance the stability of solar wind models, especially as we move toward more detailed hybrid and kinetic simulations that incorporate complex plasma physics. Many numerical models have been validated against observational data from spacecraft such as the Parker

Solar Probe, Solar Dynamic Observatory (SDO), Geostationary Operational Environmental Satellite (GOES), and the Solar and Heliospheric Observatory (SOHO). This has allowed researchers to refine their models and improve our understanding of solar wind properties.

Authors' Contributions

The author contributed to data analysis, drafting, and revising of the paper and agreed to be responsible for all aspects of this work.

Data Availability

No data available.

Conflicts of Interest

The author declares that there is no conflict of interest.

Ethical Considerations

The author has diligently addressed ethical concerns, such as informed consent, plagiarism, data fabrication, misconduct, falsification, double publication, redundancy, submission, and other related matters.

Funding

This research did not receive any grant from funding agencies in the public, commercial, or non profit sectors.

References

[1] Council, N. R., et al. 2004, Plasma physics of the local cosmos, National Academies Press.

[2] Council, N. R., et al. 2004, Solar and Space Physics and Its Role in Space Exploration, National Academies Press.

[3] Mandea, M., Korte, M., Yau, A., & Petrovsky, E. 2019, Geomagnetism, Aeronomy and Space Weather: A Journey from the Earth's Core to the Sun.

[4] Taran, S., et al. 2023, Advances in Space Research, 71, 5453.

[5] Nandy, D., et al. 2023, J. Atmospheric and Solar-Terrestrial Physics, 248, 106081.

[6] Parker, E. 1958, The Physics of Fluids, 1, 171.

[7] Echim, M. M., Lemaire, J., & Lie-Svendsen, O. 2011, Surveys in geophysics, 32, 1.

[8] Moschou, S.-P., 2016, Dynamics of the solar atmosphere and solar wind modeling.

[9] Feng, X. 2019, Magnetohydrodynamic modeling of the solar corona and heliosphere, Springer.

[10] Alberti, T., et al. 2019, Entropy, 21, 320.

[11] Davidson, P. A. 2017, Introduction to magnetohydrodynamics.

[12] Parker, E. N. 1958, ApJ, 128, 664.

[13] Lemaire, J., & Scherer, M. 1971, J. Geophysical Research, 76, 7479.

[14] Maksimovic, M., Pierrard, V., & Lemaire, J. F. 1997, Astronomy and Astrophysics, 324, 725.

[15] Marsch, E. 2018, Annales Geophysicae, Copernicus GmbH.

[16] Chaudhary, K., Imam, A. M., Rizvi, S. Z. H., & Ali, J. 2018, Kinetic Theory; InTech: Rijeka, Croatia, 107.

[17] Verscharen, D., Klein, K. G., & Maruca, B. A. 2019, Living Reviews in Solar Physics, 16, 5.

[18] Ofman, L. 2010, Living Reviews in Solar Physics, 7, 1.

[19] Perrone, D., et al. 2013, Space Science Reviews, 178, 233.

[20] Servidio, S., et al. 2015, J. Plasma Physics, 81, 325810107.

[21] Tina, G., Gagliano, S., & Raiti, S. 2006, Solar energy, 80, 578.

[22] Hughes, R. S., Ph.D. thesis, University of Southern California 2017.

[23] Winske, D., et al. 2023, Space and Astrophysical Plasma Simulation: Methods, Algorithms, and Applications.

[24] Pekünlü, E. R., Çakırlı, Ö., & Özetken, E. 2001, MNRAS, 326, 675.

[25] Nasiri, S., Safari, H., & Sobouti, Y. 2007, Solar and Stellar Physics Through Eclipses.

[26] Safari, H., Nasiri, S., & Sobouti, Y. 2007, Astronomy & Astrophysics, 470, 1111.

[27] Kozlov, D. 2010, J. atmospheric and solar-terrestrial physics, 72, 1348.

[28] Salem, C. S., et al. 2012, ApJLetters, 745, L9.

[29] Podesta, J. J. 2013, Solar Physics, 286, 529.

[30] Esmaeili, S., Nasiri, M., Dadashi, N., & Safari, H. 2015, AAS/AGU Triennial Earth-Sun Summit, Vol. 1 of AAS/AGU Triennial Earth-Sun Summit Publisher , p. 403.17.

[31] Bale, S., et al. 2016, Space science reviews, 204, 49.

[32] Kasper, J. C., et al. 2019, Nature, 576, 228.

[33] Huang, S., et al. 2020, ApJletters, 897, L3.

[34] Nakariakov, V. M., & Kolotkov, D. Y. 2020, Annual Review of Astronomy and Astrophysics, 58, 441.

[35] Ayaz, S., Li, G., & Khan, I. A. 2024, ApJ, 970, 140.

[36] Vasko, I., et al. 2024, ApJLetters, 967, L31.

[37] Arora, M., & Roe, P. L. 1997, J. Computational Physics, 130, 25.

[38] Yee, H. C. 1987, Upwind and symmetric shock-capturing schemes, National Aeronautics and Space Administration, Ames Research Center.

[39] Groth, C. P., De Zeeuw, D. L., Gombosi, T. I., & Powell, K. G. 2000, Journal of Geophysical Research: Space Physics, 105, 25053.

[40] Usmanov, A. V., Goldstein, M. L., & Matthaeus, W. H. 2014, The Astrophysical Journal, 788, 43.

[41] Guo, X., Zhou, Y., Wang, C., & Liu, Y. D. 2021, Earth and Planetary Physics, 5, 223.

[42] Varela, J., et al. 2022, Astronomy & Astrophysics, 659, A10.

[43] Baker, D. N., et al. 2013, J. Geophysical Research: Space Physics, 118, 45.

[44] van der Holst, B., et al. 2014, ApJ, 782, 81.

[45] Inc., P. S. MAS: Magnetohydrodynamic Algorithm outside a Sphere, `https://www.predsci.com/mas/`.

[46] Pomoell, J., & Poedts, S. 2018, J. Space Weather and Space Climate, 8, A35.

[47] Hinterreiter, J., et al. 2019, [arXiv:1907.07461].

[48] Li, Y., et al. 2025, [arXiv:2511.19975].

[49] Abbo, L., et al. 2016, Space Science Reviews, 201, 55.

[50] Dröge, W., Kartavykh, Y., Klecker, B., & Kovaltsov, G. 2010, ApJ, 709, 912.

[51] Horbury, T., Wicks, R., & Chen, C. 2012, Space Science Reviews, 172, 325.

[52] Dudík, J., et al. 2017, Solar Physics, 292, 1.

[53] Kulsrud, R. M. 2020, Plasma physics for astrophysics.

[54] Priest, E. 2014, Magnetohydrodynamics of the Sun, Cambridge University Press.

[55] Nordlund, Å. 2004, The Solar-B Mission and the Forefront of Solar Physics.

[56] Wang, C., et al. 2013, Science China Earth Sciences, 56, 1141.

[57] Wang, Z. 1994, Application of recently developed numerical technology to solar hydrodynamics/magnetohydrodynamics processes, University of California, Los Angeles.

[58] Johnson, N. L., Technical report, Los Alamos National Lab.(LANL), Los Alamos, NM (United States) (unpublished).

[59] Vantieghem, S. 2011, Université Libre de Bruxelles.

[60] Zank, G., & Matthaeus, W. 1992, J. geophysical research, 97, 17189.

[61] Murawski, K., & Tanaka, T. 1997, Astrophysics and space science, 254, 187.

[62] Mejnertsen, L., et al. 2018, J. Geophysical Research: Space Physics, 123, 259.

[63] Wu, S., Andrews, M., & Plunkett, S. 2001, Space Science Reviews, 95, 191.

[64] Riley, P., et al. 2003, J. Geophysical Research: Space Physics, 108.

[65] Chen, P. 2011, Living Reviews in Solar Physics, 8, 1.

[66] Zhou, Y., Feng, X., & Zhao, X. 2014, J. Geophysical Research: Space Physics, 119, 9321.

[67] Lugaz, N., Temmer, M., Wang, Y., & Farrugia, C. J. 2017, Solar Physics, 292, 1.

[68] Hudson, M. K., et al. 2021, Space weather, 19, e2021SW002882.

[69] Shen, F., et al. 2022, Reviews of Modern Plasma Physics, 6, 8.

[70] Steinolfson, R. S., & Dryer, M. 1978, J. Geophysical Research: Space Physics, 83, 1576.

[71] Wu, C.-C., Chao, J., Wu, S., & Dryer, M. 1996, Solar Physics, 165, 377.

[72] Pushkar, E. 2009, Fluid Dynamics, 44, 917.

[73] Marsch, E. 2006, Advances in Space Research, 38, 921.

[74] Chapman, S. C., Hnat, B., & Kiyani, K. 2008, Nonlinear Processes in Geophysics, 15, 445.

[75] Rouillard, A. P., et al. 2021, Solar Physics and Solar Wind, 1.

[76] Odstrcil, D. 2023, Frontiers in Astronomy and Space Sciences, 10, 1226992.

[77] Rasca, A., Horányi, M., Oran, R., & van Der Holst, B. 2014, J. Geophysical Research: Space Physics, 119, 18.

[78] Ozturk, D., Ph.D. thesis, 2018.

[79] Zhou, H., & Tóth, G. 2020, J. Parallel and Distributed Computing, 139, 65.

[80] Kuzmin, D., Löhner, R., & Turek, S. 2012, Flux-corrected transport: principles, algorithms, and applications, Springer Science & Business Media.

[81] da Silva, P. C., et al. 2024, Computational Geosciences, 1.

[82] Marsch, E. 2006, Living Reviews in Solar Physics, 3, 1.

[83] Kulsrud, R. M. 1983, Handbook of plasma physics, 1, 115.

[84] Chew, F. 1955, Eos, Transactions American Geophysical Union, 36, 963.

[85] Kulsrud, R. 1962, The Physics of Fluids, 5, 192.

[86] Chandran, B. D., Dennis, T. J., Quataert, E., & Bale, S. D. 2011, ApJ, 743, 197.

[87] Taran, S., Safari, H., & Daei, F. 2019, ApJ, 882, 157.

[88] Rudakov, L., Mithaiwala, M., Ganguli, G., & Crabtree, C. 2011, Physics of Plasmas, 18.

[89] Zong, Q. 2022, Annales geophysicae, Copernicus GmbH.

[90] Selzer, L. A., Ph.D. thesis, University of Warwick 2015.

[91] Schroeder, J. W. 2024, Alfvén Waves Across Heliophysics: Progress, Challenges, and Opportunities, 269.

[92] Majeski, S., & Kunz, M. W. 2024, J. Plasma Physics, 90, 535900101.

[93] Valentini, F., et al. 2009, Numerical Simulation Research Progress, New York: Nova Sci. Publ, 99.

[94] Bottino, A., & Sonnendrücker, E. 2015, J. Plasma Physics, 81, 435810501.

[95] Bailo, R., Carrillo, J. A., & Hu, J. 2024, [arXiv:2401.01689].

[96] Sahraoui, F., Belmont, G., & Goldstein, M. 2012, ApJ, 748, 100.

[97] Howes, G. 2015, Philosophical Transactions of the Royal Society A: Mathematical, Physical and Engineering Sciences, 373, 20140145.

[98] Huang, K., Ph.D. thesis, 2023.

[99] David, V., Ph.D. thesis, Université Paris-Saclay 2023.

[100] Yamada, M., Kulsrud, R., & Ji, H. 2010, Reviews of modern physics, 82, 603.

[101] Louarn, P., et al. 2015, Space Science Reviews, 187, 181.

[102] Pucci, F., et al. 2020, J. Plasma Physics, 86, 535860601.

[103] Izmodenov, V. V. 2018, Physics-Uspekhi, 61, 793.

[104] Korolkov, S., & Izmodenov, V. 2021, MNRAS, 504, 4589.

[105] Brandt, P., et al. 2023, Space science reviews, 219, 18.

[106] De Zeeuw, D. L., et al. 2000, IEEE Transactions on Plasma Science, 28, 1956.

[107] Goedbloed, J. P., Keppens, R., & Poedts, S. 2010, Advanced magnetohydrodynamics: with applications to laboratory and astrophysical plasmas, Cambridge University Press.

[108] Evans, G., Blackledge, J., & Yardley, P. 2012, Numerical methods for partial differential equations, Springer Science & Business Media.

[109] Hussaini, M. Y., & Zang, T. A., Technical report (unpublished).

[110] Tskhakaya, D., Matyash, K., Schneider, R., & Taccogna, F. 2007, Contributions to Plasma Physics, 47, 563.

[111] Plewa, T., et al. 2005, Adaptive mesh refinement, theory and applications, Springer.

[112] Crank, J., & Nicolson, P. 1996, Advances in Computational Mathematics, 6, 207.

[113] Cebeci, T. 2002, Convective heat transfer, Springer.

[114] Van der Holst, B., et al. 2011, ApJSupplement Series, 194, 23.

[115] Costa, J. T., Ph.D. thesis, Université Côte d'Azur 2016.

[116] Teukolsky, S. A. 2000, Phys. Rev. D, 61, 087501.

[117] Tran, Q., & Liu, J. 2016, [arXiv:1608.01344].

[118] Leiler, G., & Rezzolla, L. 2006, Phys. Rev. D, 73, 044001.

[119] Tóth, G., et al. 2005, J. Geophysical Research: Space Physics, 110.

[120] Giraldo, F. X. 2018, Time-integrators, Lecture notes.

[121] Feng, X., et al. 2010, ApJ, 723, 300.

[122] Coburn, J. T., et al. 2024, ApJ, 964, 100.

[123] Dyadechkin, S., Kallio, E., & Jarvinen, R. 2013, J. Geophysical Research: Space Physics, 118, 5157.

[124] Marsch, E., et al. 1982, J. Geophys. Res., 87, 35.

[125] Landi, E. 2008, ApJ, 685, 1270.

[126] Newbury, J., Russell, C., Phillips, J., & Gary, S. 1998, J. Geophysical Research: Space Physics, 103, 9553.